

强磁场科学研究动态监测快报



主办单位：中国科学院合肥物质科学研究院信息中心

中国科学院强磁场科学中心

目录

本期要览.....	1
世界主要强磁场实验室介绍——HFLSM.....	5
1. Introduction of HFLSM, Tohoku University	5
强磁场装置研制.....	5
1. Bi-2223 Test Coils for High-Resolution NMR Magnets.....	5
2. Research and Development of the High Stable Magnetic Field ReBCO Coil System Fundamental Technology for MRI.....	6
3. Design and Test Results of a Cryogenic Cooling System for a 25-T Cryogen-Free Superconducting Magnet	6
强磁场与材料科学.....	7
1. Ultra-robust high-field magnetization plateau and supersolidity in bond-frustrated MnCr ₂ S ₄	7
2. High field hyperpolarization-EXSY experiment for fast determination of dissociation rates in SABRE complexes	7
3. Resolution of the Two Aluminum Sites in Ettringite by Al-27 MAS and MQMAS NMR at Very High Magnetic Field (22.3 T)	8
4. Disorder-Induced Revival of the Bose-Einstein Condensation in Ni(Cl _{1-x} Br _x) ₂ -4SC(NH ₂) ₂ at High Magnetic Fields	8
5. The Zeeman splitting of bulk 2H-MoTe ₂ single crystal in high magnetic field	9
6. Optimization of thermoelectric properties in layered Bi ₂ Sr ₂ Co ₂ O _y via high-magnetic-field sintering	9
7. Magnetic properties of a Ho ₂ Fe ₁₄ Si ₃ single crystal	10
8. Effect of Simultaneous Addition of 1D and 3D Artificial Pinning Centers in Hybrid YBa ₂ Cu ₃ O _{7-x} Multilayers	10
9. Magneto-Dendrite Effect: Copper Electrodeposition under High Magnetic Field	11
10. Upper critical field reaches 90 tesla near the Mott transition in fulleride superconductors	11
11. Magnetization Process of the Kondo Insulator YbB ₁₂ in Ultrahigh Magnetic Fields	12

12.	Magnetic transitions under ultrahigh magnetic fields of up to 130 T in the breathing pyrochlore antiferromagnet $\text{LiInCr}_4\text{O}_8$	12
13.	Helium nanodroplets shed light on phase separations in other materials.....	12
强磁场与生物医学.....		14
1.	Analysis of Monoclonal Antibodies in Human Serum as a Model for Clinical Monoclonal Gammopathy by Use of 21 Tesla FT-ICR Top-Down and Middle-Down MS/MS	14
2.	27 T ultra-high static magnetic field changes orientation and morphology of mitotic spindles in human cells	14
3.	New record NMR magnet reaches peak performance.....	15
4.	"Bath salt" drugs disrupt brain activity	16

本期要览

◇ 世界主要强磁场实验室介绍——HFLSM

日本东北大学高场实验室

为了发展应用于聚变反应堆中限制等离子体超导磁体所用的超导材料，日本于 1981 年 4 月在东北大学建立了针对超导材料开发的高场实验室。该实验室的主要实验设备是一台 31T 混合磁体，该混合磁体外插超导磁体，内插功率为 8MW 的水冷磁体。同时，该实验室也发展了多台超导磁体。

日本东北大学高场实验室同时也为科研人员提供用于测量材料的各种物理特性的实验设备，日本国内的各种合作研究项目也可以在此开展。

目前，有关高温超导的基础研究和材料开发是该实验室最重要的研究方向，磁场的新应用领域也同时在该实验室实施。

◇ 强磁场装置研制

文章 1 介绍了应用于高分辨率核磁共振磁体的 Bi-2223 测试线圈。近来，通过层压高强度镍合金的方式，Bi-2223 带材的应变承受能力得到明显改进。目前，改进 Bi-2223 带材性能的开发项目正在美国高场实验室实施。五个 Bi-2223 超导线圈被制作，其中最后一个线圈被用来验证制作核磁共振线圈的可行性，该核磁共振线圈接近 1GH，10mm 均匀范围内均匀度为 1ppm。通过以上工作，希望能够验证 30T 核磁共振磁体的临界电流和应变特性。线圈将内插于美国高场实验室的 16T 的大口径磁体中进行测试。

文章 2 介绍了应用于 MRI 的高稳定磁场 REBCO 线圈基本技术的研究与开发。目前的 MRI 超导磁体使用的 NbTi 超导线需要在液氮温度下冷却。2013 年实施的高稳定 REBCO 线圈基本技术的研究和发展工程计划发展一个应用于 3T MRI 超导磁体的 REBCO 线圈，这项计划以实际应用作为最终目的。在这项工程中，将制作 300mm 孔径的高温超导测试线圈并评估其磁场性能。。这个线圈被 GM 制冷机低于 20K 的温度下冷却。将利用这个 REBCO 线圈制作 MRI 以评估其磁场的均匀度和稳定性。

文章 3 介绍了 25T 传导冷却超导磁体的低温冷却系统的设计和测试。25T 传导冷却超导磁体包含 11T 高温超导线圈和 14T 低温超导线圈。高温超导线圈具

有大约 10W 的交流损耗,被两台 GM 制冷机和氦气循环单元共同冷却到大约 10K。高温超导冷却系统在高温超导氦气循环管道和低温输气管道之间形成热交换。25T 传导冷却磁体冷却测试中,低温超导线圈和高温超导线圈在 164h (大约七天) 时间内从室温情况下分别被冷却到 4.3K 和 4.6K。

◇ 强磁场与材料科学¹

文章 1 介绍了体阻挫 MnCr_2S_4 体系中的超稳定高场磁化强度平台和磁超固体相。在超高外加磁场下,阻挫磁体可以展现出分数化的磁化强度平台,而每一个平台与磁场引起的晶格畸变来稳定的自旋图案一一相对应。最高达 60T 的磁化强度和超声实验展示了两个神奇的特点:(1) 一个与特殊自旋结构对应的极端稳定的磁化强度平台;(2) 两个中间相,显示了可能存在超固体相。磁化强度平台是由全部极化的 Cr 离子的磁矩贡献的,而没有 Mn 离子自旋的贡献。

文章 2 提出了强磁场下非对称复合物中基于同时超极化转移到衬底质子的一个新方法。之前已经展示了这些非平衡复合物对于 SABRE 对稀衬底的应用是非常重要的。结果展示出,由于 NMR 信号增强和更短的周期延迟,一系列高敏感度的 EXSY 谱可以在很短时间内被收集。

文章 3 报道了利用高磁场下 (22.3T) ^{27}Al 和 MQMAS 的 NMR 首次观察到钙矾石 ($(\text{Ca}_6[\text{Al}(\text{OH})_6]_2(\text{SO}_4)_3 \cdot 26\text{H}_2\text{O})$) 的八面体配位中的两个独立的 Al 位置。

文章 4 介绍了缺陷引起的强磁场下的 $\text{Ni}(\text{Cl}_{1-x}\text{Br}_x)_2\text{-4SC}(\text{NH}_2)_2$ 玻色-爱因斯坦凝聚的再生。基于最近的 NMR 实验,理论计算了无序的准一维 $S=1$ 的反铁磁材料 $\text{Ni}(\text{Cl}_{1-x}\text{Br}_x)_2\text{-4SC}(\text{NH}_2)_2$ 在强磁场下的一组物理条件。缺陷、化学控制的 Br 掺杂、相互作用、外加磁场的相互作用,导致了非常丰富的相图。在著名的反铁磁序的物理条件以外,一个与玻色爱因斯坦磁子凝聚相似的相,将在 H 大于 12.3T 处消失,科研人员揭示了在更高磁场接近 13.6T 时,由掺杂引起的相位相干将再次出现。

文章 5 介绍了强磁场下 2H-MoTe₂ 单晶的 Zeeman 劈裂。

文章 6 通过强磁场烧结优化层状 $\text{Bi}_2\text{Sr}_2\text{Co}_2\text{O}_y$ 的热电优值。

文章 7 在沿着易磁化轴方向下的 9T 稳态强磁场和最高 60T 的脉冲场下,测量了 $\text{Ho}_2\text{Fe}_{14}\text{Si}_3$ 晶体的磁化强度。

¹本节文章标引数字为正文英文报导序号。

文章 8 报道了 $\text{YBa}_2\text{Cu}_3\text{O}_{7-x}$ 混合多层膜的 1 维和 3 维人工钉扎中心的同时增加效应。

文章 9 介绍了在 15T 强磁场下的铜电沉积,使用了回旋磁水动态电极系统,发现一个在从氢气产生势到正偏压下奇异的树突状生长。

文章 10 介绍了富勒烯超导体的 Mott 转变附近的达 90T 的上临界场。在 Mott 绝缘体相附近,富勒烯的上临界场 H_{c2} 达到了 90T,是立方相晶体中最高的。

文章 11 报道了超强磁场下 Kondo 绝缘体 YbB_{12} 的磁化过程。

文章 12 介绍了在拥有“呼吸式”模的焦绿石反铁磁体 $\text{LiInCr}_4\text{O}_8$ 在超高磁场 130T 下的磁性转变。 $\text{LiGa}_{0.125}\text{In}_{0.875}\text{Cr}_4\text{O}_8$ 的磁化强度在 13T 以上显示出一个突然增加,意味着在四聚体单态基态和一个自旋为 1 的激发态之间存在着 2.2meV 的自旋能隙。

文章 13 利用高灵敏度,超低温核磁共振 (NMR) 技术,科学家们研究了一种氦同位素 (He-3 , 或 3He) 在另一种同位素 (He-4 , 或 4He) 中所构成的极稀溶液的相分离现象。科学家们通过研究一个替代系统,攻克了之前他们无法研究的“慢动作”——经典的金属合金中的热扩散: 3He-4He 系统中的量子扩散,其进行的速度呈数量级地提升。

◇ 强磁场与生物医学²

文章 1 利用 21T 傅里叶变换离子回旋共振质谱法 (FT-ICR) 上-下和中-下串联质谱 (MS/MS) 分析了作为临床单克隆丙种球蛋白病模型的人血清单克隆抗体。

文章 2 报道了 27T 超强稳态磁场改变人类细胞有丝分裂纺锤体的方向与形态。科研人员发现人鼻咽癌细胞 CNE-2Z 和人视网膜色素上皮细胞 RPE1 的纺锤体均在 27T 稳态磁场中重新排列。纺锤体排列的方向取决于染色体形成平面的中期板的程度。研究结果表明,磁力矩作用于微管和染色体上,而且纺锤体相对于磁场方向的排列方式取决于染色体要多于微管自身。此外,纺锤体的形态也被 27T 稳态磁场所影响。这是首次报道细胞对超过 20T 超高磁场的响应。

文章 3 报道了核磁共振 (NMR) 磁体达到的峰值性能创新纪录。2016 年, MagLab 公司的新型串联混合型 (SCH) 磁体达到 36 T 的世界纪录。最近,它在

²本节文章标引数字为正文英文报导序号。

两次实验中均达到其规格性能，且磁场变化小于百万分之一。换言之，磁场在实验进行的空间内和时间内的变化非常非常小。这种高度均匀和稳定场使得固态 NMR 实验用场强比之前高了 50%。

文章 4 揭示了“浴盐”毒品扰乱大脑活动。利用功能性磁共振成像 (fMRI)，科学家们发现其中一种最强效的浴盐毒品 (俗称摇头丸、PeeVee, 或是超级可乐) 对大鼠脑内这些信号有不利影响，最终造成大脑连接大范围紊乱。重要脑信号的中断几乎肯定会影响大脑不同区域的相互交流。摇头丸对大脑影响的直接影像可能有朝一日会促进毒瘾治疗的发展，并且能更进一步理解损伤的原因。它还将帮助人们了解浴盐毒品对大脑功能和结构短期和长期的影响。这项开创性工作利用高场成像技术加深了我们对基本脑机制的理解。

世界主要强磁场实验室介绍——HFLSM

1. Introduction of HFLSM, Tohoku University

HFLSM was established in April 1981 in order to provide research facilities for the development of superconducting materials which would be used for superconducting magnets for the plasma confinement in fusion reactors. The main equipment is a hybrid magnet which generates steady high magnetic fields up to 31 T. The hybrid magnet consists of a superconducting outer solenoid and of a water-cooled inner one with maximum steady power consumption of 8 MW. In addition superconducting magnets which has been developed by our laboratory are installed.

The laboratory also provides instruments for measuring various physical properties. These facilities are open to scientists and engineers on superconductors and other materials. Cooperative research programs are under way in a nationwide scale.

Basic research and materials developments of high-temperature superconductors are the most important research subject of this laboratory. New application research of magnetic field for materials development process is also carried out.

HFLSM research equipments as follows:

Magnet	31T-HM	28T-HM	28T-CHM	25T-CHM	20T-SM	18T-SM	15T-SM	20T-CSM	15T-CSM	10T-CSM	11T-CSM	8T-CSM	6T-CSM	5T-CSSM
Effective bore (mm)	32	52	32	52	52	52	52	52	52	100	52	220	220	52×10
Central field (T)	30	27	28	25	19.5/17.5	18	15	20	15	10	11	8	6	5
Equipments														
Magnetic levitation	○	○	○	○										
Crystal growth(heat treatment)		○		○				○	○	○				
X-ray diffraction														○
Specific heat					○									
Thermal conductivity							○							
Differential thermal analysis		○		○				○	○	○				
Low temperature	³ He	○		○	○	○	○							
	³ He/ ⁴ He			○	○	○								
Ultrasonic			△	△										
Transport properties	Resistivity	○	○	○	○	○	○	○	○	○		○	○	○
	Hall effect	○	○	○	○	○	○	○	○					
Critical current	up to 1500A	○	○	○	○									
	up to 500A	○	○	○	○		○	○	○	○		○	○	
Electrochemistry								○	○			○	○	
Optical spectroscopy	○	○	○	○		○	○							
NMR	○	○	○	○	○	○	○	○						
ESR					○	○	○							
Magnetization (Low temp.)	VSM	○	○	○	○			○	○	○				
	SEM	○	○	○	○	○	○		○	○				
	AC		○		○	○	○		○	○				
Magnetization (High temp.)		○		○				○	○	○	○			

Research equipments

Information Sources: <http://www.hflsm.imr.tohoku.ac.jp/cgi-bin/index-e.cgi>

强磁场装置研制

1. Bi-2223 Test Coils for High-Resolution NMR Magnets

Recently, significant improvement in the strain tolerance of Bi-2223 conductor has been achieved by lamination with high strength nickel alloy. The conductor, supplied by Sumitomo Electric and designated Type HT-NX, is now commercially available in lengths sufficient for manufacture of high-homogeneity solenoids. A program to fully exploit the improved conductor properties is now underway at the National High Magnetic Field Laboratory (NHMFL). Five coils are being made, the last of which is to demonstrate an NMR measurement approaching 1 GHz and 1 ppm over 10-mm volume. In so doing, we expect to demonstrate critical current fraction, and strain similar to that expected in 30-T NMR magnets. The coils will be tested inside an existing 16 Tesla large-bore background magnet at the NHMFL. The design of the NMR demonstration coil is presented first, with expected values for field, homogeneity, and strain given. A technology development program is then outlined, which includes fabrication of four test coils to test various design features, develop fabrication tooling, and train personnel.

Information Sources: <http://ieeexplore.ieee.org/stamp/stamp.jsp?arnumber=7815263>

2. Research and Development of the High Stable Magnetic Field ReBCO Coil System Fundamental Technology for MRI

The superconducting magnet is effective to get a high stable and high magnetic field for magnetic resonance imaging (MRI). The current MRI superconducting magnet needed cooling in the liquid helium (4.2 K) to use NbTi superconducting wire. In the past few years, price increase and low availability of liquid helium has become a serious problem. Under such circumstances, the development of a high-temperature superconducting (HTS) coil dispensing with liquid helium cooling is greatly desired. The research and development project of the high stable magnetic field ReBCO coil system fundamental technology that started from the latter half of 2013 develops a ReBCO coil for 3 T MRI superconducting magnets. It gets a prospect of the practical use as the final aim. In this project, we will produce an HTS test coil of 300 mm bore experimentally and evaluate the magnetic field. This coil is cooled in less than 20 K by a GM refrigerator. We are going to make MRI used by the ReBCO coil field to evaluate the uniformity and stability of the magnetic field.

Information Sources: <http://ieeexplore.ieee.org/stamp/stamp.jsp?arnumber=7801065>

3. Design and Test Results of a Cryogenic Cooling System for a 25-T Cryogen-Free Superconducting Magnet

A cryogenic cooling system for a 25-T cryogen-free superconducting magnet (25T-CSM) was developed. The 25T-CSM consisted of 11-T high-Tc superconducting (HTS) coils and 14 T low-Tc superconducting (LTS) coils. The HTS coils, which had about 10-W AC-loss, were cooled to

about 10 K by two GM cryocoolers and a helium gas circulation unit. In this system, the gas flow rate had an optimized value and was controlled by a mass flow controller. The LTS coils were cooled to about 4 K by two GM/JT cryocoolers. Each GM/JT cryocooler had two sets of precooling gas lines. These pre-cooling lines were cooled by two single-stage GM cryocoolers and the HTS coil cooling system via a heat exchanger, between the HTS gas circulation line and the LTS cool-down line. As a result of cooling test of the 25T-CSM, the LTS coils and HTS coils were cooled from room temperature to 4.3 K and 4.6 K within 164 h (about seven days), respectively. During the excitation test of the HTS coils, their maximum temperature increased to 7.6 K, which was still sufficiently low.

Information Sources: <http://ieeexplore.ieee.org/document/7862758/>

强磁场与材料科学

1. Ultra-robust high-field magnetization plateau and supersolidity in bond-frustrated MnCr_2S_4

Frustrated magnets provide a promising avenue for realizing exotic quantum states of matter, such as spin liquids and spin ice or complex spin molecules. Under an external magnetic field, frustrated magnets can exhibit fractional magnetization plateaus related to definite spin patterns stabilized by field-induced lattice distortions. Magnetization and ultrasound experiments in MnCr_2S_4 up to 60 T reveal two fascinating features: (i) an extremely robust magnetization plateau with an unusual spin structure and (ii) two intermediate phases, indicating possible realizations of supersolid phases. The magnetization plateau characterizes fully polarized chromium moments, without any contributions from manganese spins. At 40 T, the middle of the plateau, a regime evolves, where sound waves propagate almost without dissipation. The external magnetic field exactly compensates the Cr–Mn exchange field and decouples Mn and Cr sublattices. In analogy to predictions of quantum lattice-gas models, the changes of the spin order of the manganese ions at the phase boundaries of the magnetization plateau are interpreted as transitions to supersolid phases.

Information Sources: <http://advances.sciencemag.org/content/3/3/e1601982>

2. High field hyperpolarization-EXSY experiment for fast determination of dissociation rates in SABRE complexes

SABRE (Signal Amplification By Reversible Exchange) is a nuclear spin hyperpolarization technique based on the reversible concurrent binding of small molecules and para-hydrogen (p-H₂) to an iridium metal complex in solution. At low magnetic field, spontaneous conversion of

p-H-2 spin order to enhanced longitudinal magnetization of the nuclear spins of the other ligands occurs. Subsequent complex dissociation results in hyperpolarized substrate molecules in solution. The lifetime of this complex plays a crucial role in attained SABRE NMR signal enhancements. Depending on the ligands, vastly different dissociation rates have been previously measured using EXSY or selective inversion experiments. However, both these approaches are generally time-consuming due to the long recycle delays (up to 2 min) necessary to reach thermal equilibrium for the nuclear spins of interest. In the cases of dilute solutions, signal averaging aggravates the problem, further extending the experimental time. Here, a new approach is proposed based on coherent hyperpolarization transfer to substrate protons in asymmetric complexes at high magnetic field. We have previously shown that such asymmetric complexes are important for application of SABRE to dilute substrates. Our results demonstrate that a series of high sensitivity EXSY spectra can be collected in a short experimental time thanks to the NMR signal enhancement and much shorter recycle delay.

Information Sources: <http://www.sciencedirect.com/science/article/pii/S1090780717300186>

3. Resolution of the Two Aluminum Sites in Ettringite by ^{27}Al MAS and MQMAS NMR at Very High Magnetic Field (22.3 T)

Ettringite ($\text{Ca}_6[\text{Al}(\text{OH})_6]_2(\text{SO}_4)_3 \cdot 26\text{H}_2\text{O}$) is the first hydration product formed during Portland cement hydration. ^{27}Al MAS NMR has been used in a wide number of studies to detect and quantify ettringite in hydrated cement blends by the observation of a single, narrow resonance at 13-14 ppm. This work reports the first observation of resonances from two distinct Al sites in octahedral coordination for ettringite, employing ^{27}Al MAS and MQMAS NMR at an ultrahigh magnetic field (22.3 T). Thereby, the ^{27}Al NMR spectra are in agreement with the most accepted trigonal model for the ettringite structure. ^{27}Al quadrupole coupling parameters and isotropic chemical shifts for the two Al sites are determined from simulations and least-squares optimization of slow-speed ^{27}Al MAS NMR spectra of the satellite transitions. These data reveal that the local environments for the two octahedral Al sites are very similar, in accord with the most recent XRD refinements of the ettringite structure. Finally, the significant improvement in spectral resolution by the application of an ultrahigh magnetic field is illustrated by the detection of the two Al sites from ettringite in a hydrated cement mimicking the composition of a calcium sulfoaluminate cement.

Information Sources: <http://pubs.acs.org/doi/pdf/10.1021/acs.jpcc.6b11875>

4. Disorder-Induced Revival of the Bose-Einstein Condensation in $\text{Ni}(\text{Cl}_{1-x}\text{Br}_x)_2\text{-4SC}(\text{NH}_2)_2$ at High Magnetic Fields

Building on recent NMR experiments [A. Orlova et al., Phys. Rev. Lett. 118, 067203 (2017).], we theoretically investigate the high magnetic field regime of the disordered quasi-one-dimensional $S = 1$ antiferromagnetic material $\text{Ni}(\text{Cl}_{1-x}\text{Br}_x)_2 \cdot 4\text{SC}(\text{NH}_2)_2$. The interplay between disorder, chemically controlled by Br-doping, interactions, and the external magnetic field, leads to a very rich phase diagram. Beyond the well-known antiferromagnetically ordered regime, an analog of a Bose condensate of magnons, which disappears when $H \geq 12.3$ T, we unveil a resurgence of phase coherence at a higher field H similar to 13.6 T, induced by the doping. Interchain couplings stabilize the finite temperature long-range order whose extension in the field-temperature space is governed by the concentration of impurities x . Such a "minicondensation" contrasts with previously reported Bose-glass physics in the same regime and should be accessible to experiments.

Information Sources: <https://journals.aps.org/prl/abstract/10.1103/PhysRevLett.118.067204>

5. The Zeeman splitting of bulk 2H-MoTe₂ single crystal in high magnetic field

A high magnetic field magneto-optical spectrum is utilized to study the A exciton of bulk 2H-MoTe₂ single crystal. A clear Zeeman splitting of the A exciton is observed under high magnetic fields up to 41.68T, and the g-factor (-2.09 +/- 60.08) is deduced. Moreover, a high magnetic field enables us to obtain the quadratic diamagnetic shifts of the A exciton (0.486 mu eV T⁻²). Accordingly, the binding energy, reduced mass, and radius of the A exciton were obtained by using both two and three dimensional models. Compared with other transition metal dichalcogenides (TMDs), the A exciton of bulk 2H-MoTe₂ has a relatively small binding energy and larger exciton radius, which provide fundamental parameters for comprehensive understanding of excitons in TMDs as well as their future applications.

Information Sources: <http://aip.scitation.org/doi/pdf/10.1063/1.4977953>

6. Optimization of thermoelectric properties in layered Bi₂Sr₂Co₂O_y via high-magnetic-field sintering

Herein, we report the effect of the high-magnetic-field (HMF) sintering on the structural, electrical and thermal transport properties of the layered Bi₂Sr₂Co₂O_y. Based on the results of x-ray diffraction and microtopography, we find the grains prefer to the oriented growth along the direction of applied magnetic field, leading to a higher textured degree and anisotropy. Correspondingly, the in-plane conductivity increases while the out-of-plane one reduces with increasing sintering magnetic field. At the same time, the in-plane thermopower shows an obvious enhancement after the HMF sintering, which mainly originates in the spin state transition of Co⁴⁺

ions. As a result, a remarkable enhancement of the in-plane thermoelectric figure-of-merit is obtained in the sample after the HMF sintering (8 T).

Information Sources: <http://www.sciencedirect.com/science/article/pii/S092583881730542X>

7. Magnetic properties of a $\text{Ho}_2\text{Fe}_{14}\text{Si}_3$ single crystal

Magnetization of a $\text{Ho}_2\text{Fe}_{14}\text{Si}_3$ single crystal was measured in a steady magnetic field of up to 9 T and in pulsed fields of up to 60 T applied along the principal axes. $\text{Ho}_2\text{Fe}_{14}\text{Si}_3$ is a ferrimagnet below $T_c = 480$ K, has a spontaneous magnetic moment of about 8 μ_B /f.u. (at $T = 4.2$ K) and exhibits a large easy-plane magnetic anisotropy. There is also a certain anisotropy within the basal plane, the b axis [120] being the easy-magnetization direction. In fields applied along the a and b axes field-induced first-order phase transitions are observed at 29 T and at 22 T, respectively. Along the easy axis b we observe also an S-shaped anomaly at about 47 T, which does not correspond to a phase transition. A simple model predicts that the two observed first-order transitions are the only ones taking place in $\text{Ho}_2\text{Fe}_{14}\text{Si}_3$; the magnetization should subsequently grow continuously and arrive at saturation at similar to 100 T. This is in stark contrast to the behavior of the parent compound $\text{Ho}_2\text{Fe}_{17}$, where as many as three sequential first-order transitions are expected for H parallel to b. The reason for the disparity is that the basal-plane anisotropy constant K_{Ho} is at least one order of magnitude smaller in $\text{Ho}_2\text{Fe}_{14}\text{Si}_3$ than it is in $\text{Ho}_2\text{Fe}_{17}$.

Information Sources: <http://www.sciencedirect.com/science/article/pii/S0925838816331772>

8. Effect of Simultaneous Addition of 1D and 3D Artificial Pinning Centers in Hybrid $\text{YBa}_2\text{Cu}_3\text{O}_{7-x}$ Multilayers

The nanoengineering approach by PLD method can produce a variety of complex nanocomposite oxide thin films with unique properties for sustainable applications. We report on the epitaxial growth and superconducting properties of $\text{YBa}_2\text{Cu}_3\text{O}_{7-x}$ (YBCO) multilayers incorporating BaSnO_3 (BSO) nanorods and Y_2O_3 nanoparticles at the same time in order to combine the advantages of both columnar (1D, BSO) and isotropic (3D, Y_2O_3) pinning with the purpose of enhance the pinning force of the films for a wide range of applications in large external magnetic fields. Multilayered films, alternating YBCO+ Y_2O_3 and YBCO+ BSO layers were grown in pulsed laser deposition chamber by switching a surface-modified YBCO+similar to 2A% Y_2O_3 target and a mixed YBCO+ 4 wt% BSO target. Different combinations for films' growth have been tried via varying the thickness of the alternating layers. The best result was obtained with the combination [(90 nm YBCO+ BSO)/(30 nm YBCO+ Y_2O_3)] x3 presenting a maximum

global pinning force $F_p(\text{max}) = 17.6 \text{ GN/m}^3$ (77 K, 2.2 T, B//c), more than 3 times larger than for typical pure YBCO films. These results demonstrate that the nanoengineering approach is at very advanced level: satisfactory control of nanodefects size and distribution was achieved. At the end, a renewed approach based on the Ginzburg-Landau single vortex theory is used to discuss the contributions of 1D, 3D and 1D+ 3D APCs to the global pinning force of the hybrid multilayers.

InformationSources: <http://chinesesites.library.ingentaconnect.com/content/asp/sam/2017/00000009/00000006/art00028;jsessionid=aqpb7mlq6f26s.x-ic-live-01>

9. Magneto-Dendrite Effect: Copper Electrodeposition under High Magnetic Field

Ionic vacancy is a by-product in electrochemical reaction, composed of polarized free space of the order of 0.1 nm with a 1 s lifetime, and playing key roles in nano-electrochemical processes. However, its chemical nature has not yet been clarified. In copper electrodeposition under a high magnetic field of 15 T, using a new electrode system called cyclotron magnetohydrodynamic (MHD) electrode (CMHDE) composed of a pair of concentric cylindrical electrodes, we have found an extraordinary dendritic growth with a drastic positive potential shift from hydrogen-gas evolution potential. Dendritic deposition is characterized by the co-deposition of hydrogen molecule, but such a positive potential shift makes hydrogen-gas evolution impossible. However, in the high magnetic field, instead of flat deposit, remarkable dendritic growth emerged. By examining the chemical nature of ionic vacancy, it was concluded that ionic vacancy works on the dendrite formation with the extraordinary potential shift.

InformationSources: <https://www.nature.com/articles/srep45511>

10. Upper critical field reaches 90 tesla near the Mott transition in fulleride superconductors

Controlled access to the border of the Mott insulating state by variation of control parameters offers exotic electronic states such as anomalous and possibly high-transition-temperature (T_c) superconductivity. The alkali-doped fullerides show a transition from a Mott insulator to a superconductor for the first time in three-dimensional materials, but the impact of dimensionality and electron correlation on superconducting properties has remained unclear. Here we show that, near the Mott insulating phase, the upper critical field H_{c2} of the fulleride superconductors reaches values as high as similar to 90 T-the highest among cubic crystals. This is accompanied by a crossover from weak-to strong-coupling superconductivity and appears upon entering the metallic state with the dynamical Jahn-Teller effect as the Mott transition is approached. These results suggest that the cooperative interplay between molecular electronic structure and strong

electron correlations plays a key role in realizing robust superconductivity with high- T_c and high- H_{c2} .

Information Sources: <http://www.nature.com/articles/ncomms14467>

11. Magnetization Process of the Kondo Insulator YbB_{12} in Ultrahigh Magnetic Fields

The magnetization process of the Kondo insulator YbB_{12} has been unveiled in ultrahigh magnetic fields of up to 120 T at 4.2 K. We have found a novel metamagnetic transition at $B_{c2} = 102$ T in addition to the previously known transition at $B_{c1} = 55$ T. It has also been observed that the magnetization tends to saturate at around 112 T. Within the rigid band model, the two-energy-gap structure in the density of states (DOS) explains the successive two-step metamagnetism as a result of the Zeeman effect of the DOS. The metamagnetic transition at B_{c1} occurs along with an insulator–metal transition and the field-induced phase is expected to be a heavy fermion metallic state. The Kondo effect can weaken at the second transition of B_{c2} , as theoretically found in the successive two-metamagnetic-transition process in the Kondo semimetal CeNiSn .

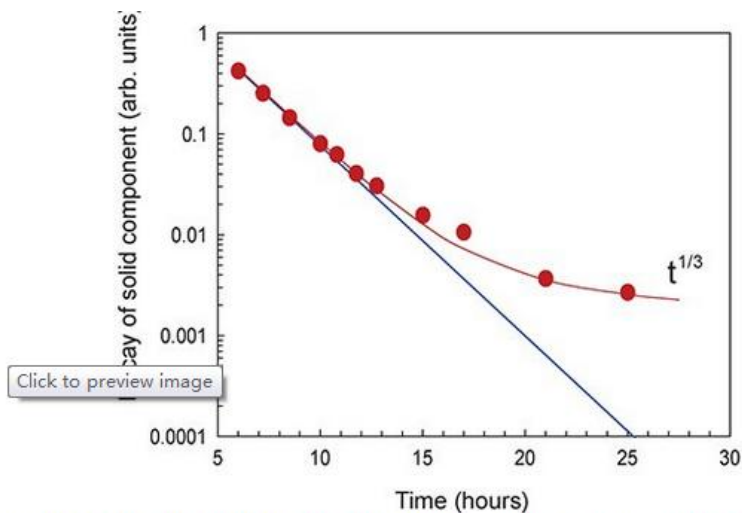
Information Sources: <http://journals.jps.jp/doi/abs/10.7566/JPSJ.86.054710>

12. Magnetic transitions under ultrahigh magnetic fields of up to 130 T in the breathing pyrochlore antiferromagnet $\text{LiInCr}_4\text{O}_8$

The magnetization processes of the spin-3/2 antiferromagnet $\text{LiInCr}_4\text{O}_8$ comprising a “breathing” pyrochlore lattice, which is an alternating array of small and large tetrahedra, are studied under ultrahigh magnetic fields of up to 130 T using state-of-the-art pulsed magnets. A half magnetization plateau is observed above 90 T to 130 T, suggesting that $\text{LiInCr}_4\text{O}_8$ has a strong spin-lattice coupling, similar to conventional chromium spinel oxides. The magnetization of $\text{LiGa}_{0.125}\text{In}_{0.875}\text{Cr}_4\text{O}_8$, in which the structural and magnetic transitions at low temperatures have been completely suppressed, shows a sudden increase above 13 T, indicating that a spin gap of 2.2 meV exists between a tetramer singlet ground state and an excited state with total spin 1, with the latter being stabilized by the application of a magnetic field. The breathing pyrochlore antiferromagnet is found to be a unique frustrated system with strong spin-lattice coupling and bond alternation.

Information Sources: <http://journals.aps.org/prb/abstract/10.1103/PhysRevB.95.134438>

13. Helium nanodroplets shed light on phase separations in other materials



Long-time decay of the NMR amplitude arising from solid helium-three that tracks the loss of the solid component to the formation of degenerate Fermi liquids in nanodroplets.

Observing growth processes in classical alloys is extremely difficult; scientists overcame this by studying quantum systems.

Phase separations are fundamentally important in condensed matter physics because they play a major role in the preparation of new materials, including high-strength metal alloys. However, these transitions occur in a kind of "slow motion" — typically over days or years. This makes them hard to measure and limits what we know about phase separations in these materials.

Scientists decided to look at *phase separations in quantum fluids* in order to shed light on *aclassical* phase transition, thermal diffusion in metallic alloys.

Using high-sensitivity, ultra-low-temperature nuclear magnetic resonance (NMR) techniques, the scientists studied the phase separation of very dilute solutions of one kind of helium isotope (helium-3, or ^3He) in another (helium-4, or ^4He).

At densities as low as 16 parts (of ^3He) per million (of ^4He), the ^3He atoms formed tiny "nanodroplets." The smallest droplets slowly shrunk as ^3He atoms diffused through the solid ^4He matrix, causing the small droplets to form larger droplets. In this so-called "coarsening" period (known as "Ostwald ripening"), the growth rate of the droplet size (and hence the decay rate of the NMR signal) is determined by the capture at the surface of the droplet, which leads to a one-third power law as a function of time.

Scientists overcame their inability to study "slow-motion," classical thermal diffusion in metallic alloys by studying a surrogate system: quantum diffusion in ^3He - ^4He , which occurs orders of magnitude faster.

Information Sources:

<https://nationalmaglab.org/user-facilities/high-b-t-facility/publications-high-bt/highlights-high-bt/solid-helium-solutions>

强磁场与生物医学

1. Analysis of Monoclonal Antibodies in Human Serum as a Model for Clinical Monoclonal Gammopathy by Use of 21 Tesla FT-ICR Top-Down and Middle-Down MS/MS

With the rapid growth of therapeutic monoclonal antibodies (mAbs), stringent quality control is needed to ensure clinical safety and efficacy. Monoclonal antibody primary sequence and post-translational modifications (PTM) are conventionally analyzed with labor-intensive, bottom-up tandem mass spectrometry (MS/MS), which is limited by incomplete peptide sequence coverage and introduction of artifacts during the lengthy analysis procedure. Here, we describe top-down and middle-down approaches with the advantages of fast sample preparation with minimal artifacts, ultrahigh mass accuracy, and extensive residue cleavages by use of 21 tesla FT-ICR MS/MS. The ultrahigh mass accuracy yields an RMS error of 0.2–0.4 ppm for antibody light chain, heavy chain, heavy chain Fc/2, and Fd subunits. The corresponding sequence coverages are 81%, 38%, 72%, and 65% with MS/MS RMS error ~4 ppm. Extension to a monoclonal antibody in human serum as a monoclonal gammopathy model yielded 53% sequence coverage from two nano-LC MS/MS runs. A blind analysis of five therapeutic monoclonal antibodies at clinically relevant concentrations in human serum resulted in correct identification of all five antibodies. Nano-LC 21 T FT-ICR MS/MS provides nonpareil mass resolution, mass accuracy, and sequence coverage for mAbs, and sets a benchmark for MS/MS analysis of multiple mAbs in serum. This is the first time that extensive cleavages for both variable and constant regions have been achieved for mAbs in a human serum background.

Information Sources: <https://link.springer.com/article/10.1007%2Fs13361-017-1602-6>

2. 27 T ultra-high static magnetic field changes orientation and morphology of mitotic spindles in human cells

Purified microtubules have been shown to align along the static magnetic field (SMF) in vitro because of their diamagnetic anisotropy. However, whether mitotic spindle in cells can be aligned by magnetic field has not been experimentally proved. In particular, the biological effects of SMF of above 20 T (Tesla) have never been reported. Here we found that in both CNE-2Z and RPE1 human cells spindle orients in 27 T SMF. The direction of spindle alignment depended on the extent to which chromosomes were aligned to form a planar metaphase plate. Our results show that the magnetic torque acts on both microtubules and chromosomes, and the preferred direction of spindle alignment relative to the field depends more on chromosome alignment than microtubules. In addition, spindle morphology was also perturbed by 27 T SMF. This is the first

reported study that investigated the cellular responses to ultra-high magnetic field of above 20 T. Our study not only found that ultra-high magnetic field can change the orientation and morphology of mitotic spindles, but also provided a tool to probe the role of spindle orientation and perturbation in developmental and cancer biology.

Information Sources: <https://elifesciences.org/articles/22911>

3. New record NMR magnet reaches peak performance

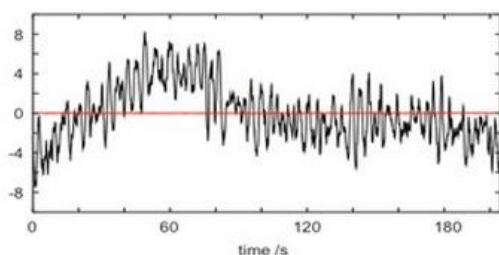


Fig. 1: Stabilizing the magnetic field at 35.2T. Black line records the way the magnetic field changes in the original configuration of the magnet at one point in space as time passes (16 ppm variation). The <0.1ppm red trace is the resulting stability after employing the temporal stabilization system.

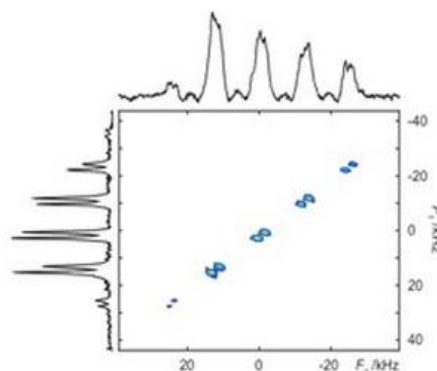


Fig. 2: Two dimensional triple quantum Magic Angle Spinning (MAS) spectra of ^{17}O benzoic acid at 35.2 T. This spectrum correlates the triple quantum signal (F_1 axis) with the single quantum spectrum (F_2 axis).

Producing a high magnetic field that is also very stable and uniform, the unique Series Connected Hybrid magnet is being put to work on NMR experiments never before possible.

Scientists can use nuclear magnetic resonance (NMR) to develop and characterize novel materials and to study chemical and biological systems. Using NMR's magnetic fields and radio waves, they pinpoint targeted elements in these materials and systems to better understand them. However, many elements in the periodic table — so-called quadrupolar nuclei — are exceptionally difficult to study using commercially-available NMR instruments because the signals they give off at those fields overlap each other.

In 2016, the MagLab's new Series Connected Hybrid (SCH) magnet reached its world-record magnetic field of 36 teslas. More recently, it attained its performance specification of less than 1 part per million of field variation in both time (a property called stability, as shown in Fig. 1) and space a property called homogeneity, as shown in Fig. 2). In other words, the magnetic field varies very, very little across the volume in which experiments are conducted and the time during which they take place. This highly uniform and stable field enables solid-state NMR experiments at 50 percent higher field than previously possible.

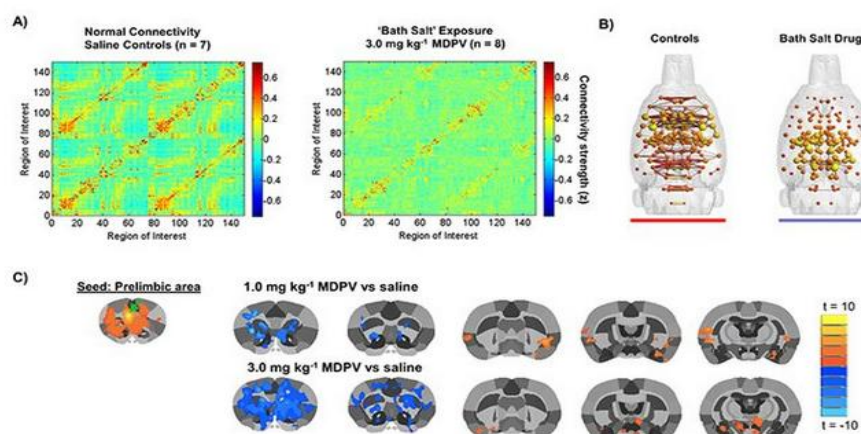
This high-field system, designed and built at the MagLab, will allow scientists to detect important quadrupolar nuclei such as oxygen, leading to new discoveries related to life and

materials.

Information Sources:

<https://nationalmaglab.org/magnet-development/magnet-science-technology/publications-ms/t/highlights-mst/world-first-1-5-ghz-nmr-magnet>

4. "Bath salt" drugs disrupt brain activity



3,4-methylenedioxypropylvalerone (MDPV) dose-dependently reduces functional connectivity with the nucleus accumbens (NAc)

Using functional magnetic resonance imaging, researchers observe how cocaine-like drug disrupts neural activity in rats.

The abuse of synthetic street drugs known as "bath salts" are a global health problem, with new variants emerging all the time. These are not the anodyne Epsom salts used for bathing, but rather potent, cocaine-like drugs.

At rest, the brain emits neural signals that reflect communication between different brain regions. Using functional magnetic resonance imaging (fMRI), scientists observed that one of the most potent bath salt drugs (known as MDPV, PeeVee, or Super Coke) adversely affected these signals in rats, causing widespread disruption in brain connectivity.

Disruption of important brain signals will almost certainly affect how different regions of their brains communicate with each other. It may even affect drug users' abilities to comprehend their surroundings while intoxicated. Direct imaging of MDPV's effects in the brain may one day lead to the development of treatments for intoxication and an understanding of the causes of impairments. It will also help inform the public on the short- and long-term effects of bath salts on brain function and structure. This pioneering work using high-field imaging techniques adds to our understanding of basic brain mechanisms.

Information Sources:

<https://nationalmaglab.org/user-facilities/nmr-mri/publications-nmr-mri/highlights-amris/bath-salt-brain-activity>

编撰： 张曙张甫许惠青代恩梅
张怡冰周丹丹陆水李玲

审稿专家： 申飞（研究员）
朱相德（副研究员）
蒋冬辉（助理研究员）
张磊（博士）

版权及合理使用声明

中国科学院合肥物质科学研究院信息中心和中国科学院强磁场科学中心主办的《强磁场科学研究动态监测快报》遵守国家知识产权法律相关规定，保护知识产权，保障著作权人的合法权益。要求参阅人员认真遵守中国著作权法的有关规定，严禁将《强磁场研究动态监测快报》用于任何商业或其他营利性用途。用于读者个人学习、研究目的单篇稿件使用时，应注明版权信息和信息来源。任何单位需要整期转载、链接或发布《强磁场科学研究动态监测快报》的内容，应向《强磁场科学研究动态监测快报》联系人发送需求函，说明用途，征得同意。

欢迎为《强磁场科学研究动态监测快报》提供意见与建议。

联系方式

邮箱：shenfei@iim.ac.cn

电话：0551-65595332